Although the early effort, as represented by all examples cited, utilized the bulk approach in waveguide components, such use is not restricted to that transmission medium. In fact, considerable effort is currently being devoted to the incorporation of such bulk semiconductor elements in various forms of TEM configurations to yield appropriately higher power greater bandwidth components. Results of this work will be forthcoming in the near future.

Finally, in fully assessing the substantial performance gains being made by the application of bulk semiconductor phenomena to control components at microwave frequencies, it should be emphasized that this approach will be even more attractive in the millimeter wave region. At such high frequencies, fabrication of useful elements other than distributed or bulk ones is impractical if not impossible. The domination of this higher frequency range with the bulk approach, at least utilizing semiconductors, is therefore assured. Some work is currently in progress on initial control components for this increasingly important millimeter wave region.

References

[1] J. Gremillet, "Isolators using semiconductors," presented at the Int. Solid-State Circuit Conf., Philadelphia, Pa., 1965.

[2] P. W. Staecker and P. Das, "Hot electron microwave rotator," *Proc. IEEE* (Corresp.), vol. 53, Nov. 1965, pp. 1766–1768.

[3] M. Todda, "A new isolator using a solid-state plasma waveguide," *IEEE Trans. Microwave Theory Tech.* (Corresp.), vol. MTT-13, Jan. 1965, pp. 126–127.

[4] H. J. Kuno and W. D. Hershberger, "Observation of microwave Faraday rotation in a solid-state plasma," *Proc. IEEE* (Lett.), vol. 57, July 1966, pp. 978–979.

[5] N. Scalar and E. Burstein, "Impact ionization of impurities in germanium," *J. Phys. Chem. Solids*, vol. 2, 1957, p. 2.

[6] J. N. Park, K. Rose, and K. E. Mortenson, "Avalanche breakdown effects in near-intrinsic silicon and germanium," *J. Appl. Phys.*, vol. 38, 1967, p. 5343.

[7] K. E. Mortenson and J. F. White, "Nonrefrigerated bulk-semiconductor microwave limiters," *IEEE J. Solid-State Circuits*, vol. SC-3, Mar. 1968, pp. 5–11.

[8] D. Leenov, "The silicon PIN diode as a microwave radar protector at megawatt levels," *IEEE Trans. Electron Devices*, vol. ED-11, Feb. 1964, pp. 53–61.

[9] K. E. Mortenson, J. M. Borrego, P. E. Bakerman, Jr., and R. J. Gutmann, "Microwave silicon windows for high-power broad-band switching applications," *IEEE J. Solid-State Circuits*, vol. SC-4, Dec. 1969, pp. 413–421.

[10] C. G. Montgomery, R. H. Dicke, and E. M. Purcell, Eds., *Principles of Microwave Circuits*, M.I.T. Rad. Lab. Ser., vol. 8. New York: McGraw-Hill, 1948, ch. 9.

[11] K. E. Mortenson, "Analysis of the temperature rise in PIN diodes caused by microwave pulse dissipation," *IEEE Trans. Electron Devices*, vol. ED-13, Mar. 1966, pp. 305–314.

[12] W. W. Mumford, "Maximally flat filters in waveguide," *Bell Syst. Tech. J.*, vol. 27, 1951, pp. 684–713.

[13] M. E. Hines, "Fundamental limitations in RF switching and phase shifting using semiconductor diodes," *Proc. IEEE*, vol. 52, June 1964, pp. 697–708.

[14] P. Cottrell, "Characterization of an iris mounted PIN switch at *X*-band," Master of Engineering Project Rep., Rensselaer Polytech. Inst., June 1970.

[15] J. F. White, "High power *p-i-n* diode controlled, microwave transmission phase shifters," *IEEE Trans. Microwave Theory Tech.*, vol. MTT-13, Mar. 1965, pp. 233–242.

[16] W. J. Ince and D. H. Temme, "Phasers and time delay elements," M.I.T. Lincoln Labs., Lexington, Mass., Project Dept. Rep. RDT-14, July 11, 1967.

[17] R. W. Burns and L. Stark, "PIN diodes advance high power phase shifting," *Microwaves*, 1965, pp. 38–48.

[18] J. F. White, "Review of semiconductor microwave phase shifters," *Proc. IEEE*, vol. 56, Nov. 1968, pp. 1924–1931.

Applications of Integrated Circuit Technology to Microwave Frequencies

HAROLD SOBOL, SENIOR MEMBER, IEEE

Abstract—Integration techniques suitable for microwave circuits have been developed. Various aspects of the technology of integration of microwave circuits are reviewed and the reasons for choosing the hybrid approach instead of the monolithic approach and thin-film metallization instead of thick-film are discussed. Design data relating circuit performance to substrate roughness and thickness of thin-film metal adhesion layers are presented. Propagation and radiation characteristics of microstrip lines are discussed. Design equations for thin-film lumped-element passive components are given. Examples of various microwave integrated circuits are shown.

Introduction

THE PAST several years have witnessed rapid progress in solid-state devices for microwave and millimeter wave applications. Avalanche and transferred electron diodes have produced watts of CW power and kilowatts of pulsed power. Microwave transistors are available as power amplifiers at *S* band and as small signal amplifiers at *C* band. Significant advances also have been made in Schottky barrier, varactor, and PIN diodes.

The solid-state device is usually fabricated as a semiconducting chip or die with a volume of the order of 500–5000 cubic milli-inches. This very small size leads to electrical, thermal, and mechanical problems. The task of applying signals to and extracting output power from the chips is by no means trivial. The parasitic reactance encountered in connecting the active device to a circuit can seriously limit the performance. Adequate heat sinking must be provided to prevent the dissipated power from excessively heating the devices and consequently degrading performance and reliability. The semiconductor die requires specialized handling techniques and protection to prevent mechanical and environmental damage.

The conventional method of treating the electrical, thermal, and mechanical problems is to mount and bond the active die in a suitably designed coaxial, pill, stripline, or microstrip package. The packaged device is then incorporated in an appropriate circuit. The use of discrete devices in conventional waveguide, coaxial or stripline circuits, suffices for many applications but leaves much to be

Manuscript received January 7, 1971.

The author is with the RCA Corporation, David Sarnoff Research Center, Princeton, N. J. 08540.

desired in others. The transverse dimensions of most conventional circuitry is much greater than the packaged device dimensions and discontinuities are introduced that limit performance. In addition, the large size and expensive machining or electroforming of conventional circuitry are undesirable in many applications. The reliability and mechanical integrity of conventional microwave circuitry is a matter of concern in certain space and military applications that require meeting severe vibration, shock, and temperature specifications. Large subassemblies that are bolted together cannot easily meet these requirements.

Many of the circuit-device interface problems and the size and cost problems of the discrete device and conventional circuit approach can be solved by utilizing microelectronic techniques for microwave circuits. Integrated circuits have revolutionized the low frequency domain because of their ability to solve these very problems. During the past several years, the microwave industry has been very active in introducing integration into the microwave bands. At this time, nearly every low and medium power microwave function has been demonstrated utilizing microwave integrated circuits (MICs). This paper will discuss the integration techniques, circuit forms and technology used for MICs, and will present examples of various devices and subsystems.

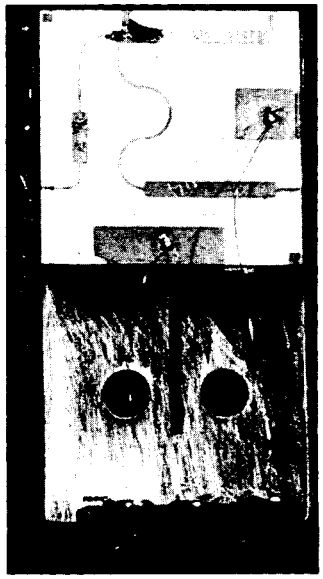

Fig. 1. *L*-band microstrip transistor amplifier, 1 by 1 by 0.010 in alumina substrate, Cr–Au lines and ground plane.

Integration Techniques

MICs like lower frequency integrated circuits (ICs) can be made in monolithic or hybrid form. In the monolithic circuit, active devices are grown *in situ* on or in a semiconducting substrate, and passive circuitry is either deposited on the substrate or grown in it. In the hybrid circuit, active devices are attached to a ceramic, glass, or ferrite substrate, containing the passive circuitry. Monolithic ICs have been successful for digital and linear applications where all required circuit components can be simultaneously fabricated. In many cases, the same device (bipolar or MOS transistors) can be utilized for amplifiers, diodes, resistors, and capacitors with no loss in performance. Many digital circuits require large arrays of identical devices. Thus it is possible in conventional ICs to obtain very high packing densities and associated low cost.

Microwave circuits are quite different from lower frequency circuits. There are very few applications that require densely packed arrays of identical devices and there is little opportunity to utilize active devices for passive components. Digital and video circuits require the storage of only potential energy and consequently no inductors are needed. Most microwave applications demand band definition and this necessitates storage of kinetic as well as potential energy; thus the packing density of typical microwave circuits (measured in terms of active real-estate to total real-estate) is far less than in conventional digital ICs. As an example, a typical microwave transistor amplifier utilizes only 5 percent of the area for the active device. One hundred of these amplifiers can be simultaneously fabricated on a 1-in silicon wafer. The same wafer on the other hand could accommodate more than 2000 transistors. If an overall yield of 10 percent is achieved, a wafer could yield 200 transistors or ten single-stage monolithic amplifiers. It is not apparent that the monolithic approach will offer any cost advantage in microwave circuits. Further, since devices are grown in or on the substrate, it is necessary to use top contact devices which can be a disadvantage in certain applications.

Subsystems for low frequency or digital applications can usually be constructed with similar devices for many of the functions. On the other hand, a microwave subsystem usually requires a variety of devices. One approach to monolithic subsystems would be to use identical processing (epitaxy, diffusions) for all devices, but to use various surface geometries. As an example, a family of PIN diodes could be used for IMPATT, switching, and tuning varactor applications. Most likely such an approach would not lead to optimum performance as too many comprises would be involved. Furthermore, while it is theoretically possible to grow GaAs on Si and vice versa, it is not practical at this time; therefore, optimum combinations of materials could not be utilized in the monolithic subsystem.

Thus it appears that conceptually, the monolithic approach is not well suited for microwave subsystems and circuits. In addition to the problems discussed previously, process difficulties, low yields, and poor performance have seriously limited the application of the monolithic technology to microwave circuits.

The hybrid technology permits the use of many varieties of devices and overcomes many of the difficulties of the monolithic technology. To date, the hybrid form of technology is used almost exclusively in the frequency range from 1 to 15 GHz. However, the monolithic technology has potential advantages that warrant consideration for future applications. A most important advantage of the monolithic approach is the reduction and control of the parasitic inductance encountered in joining the circuit and the device. This advantage is extremely important at high frequencies and makes the monolithic circuit appear attractive for millimeter-wave circuits. The main emphasis of the present paper is on the hybrid approach.

Circuit Techniques

Considerable cost reduction of passive circuitry can be achieved by the use of microelectronic techniques in place of the conventional circuit fabrication by machining and electroforming. Photolithography and screening are the most popular methods of defining circuitry for hybrid integrated circuits. In order to realize the full potential of these techniques, it is necessary to use circuit forms in which the propagation properties are determined by the definition of conductors and circuit elements in a single plane.

The microstrip transmission line shown in the transistor amplifier of Fig. 1 is the most popular form of circuit for MICs. The line consists of a strip conductor separated from the ground plane by a dielectric layer. All circuit definition is performed in the plane of the strip conductor. The impedance and length of the lines determine the circuit properties. The major part of the propagating field is confined to the region of the dielectric below the strip conductor and the propagation approximates a TEM mode.

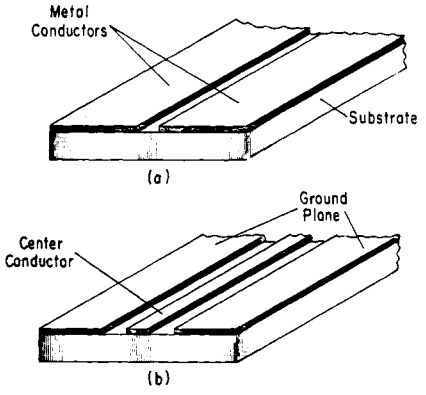

Fig. 2. Non-TEM lines for microwave integrated circuits. (a) Slotline. (b) Coplanar waveguide.

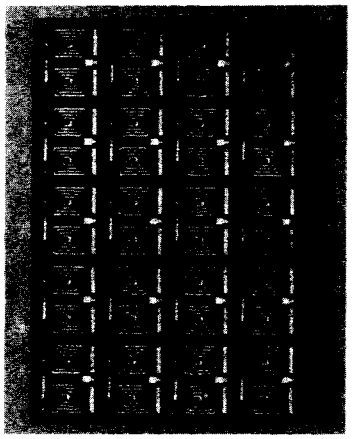

Fig. 3. Array of 3-part UHF lumped element hybrids on 1 by 0.75-in sapphire substrate, Cr–Au lines and inductors and SiO_2 capacitors.

Two other forms of distributed circuits that have recently been introduced are illustrated in Fig. 2. Fig. 2(a) illustrates the slot line [1], and Fig. 2(b) the coplanar waveguide line [2]. Because both these lines have conductors on only one side of the substrate, they generally permit shunt mounting of devices without requiring holes through the substrate, as in the case of microstrip lines. They also have longitudinal as well as transverse RF magnetic fields, and have polarization properties that are useful for nonreciprocal ferrite devices. At this time, these lines have not yet been used to the same extent as microstrip. Some interesting circuits made by combining the circuits of Fig. 2(a) and (b) with microstrip lines have been described [3].

Conventional stripline circuits are usually defined by photolithography and can be considered as a class of hybrid integrated circuits. Stripline systems that qualify as MICs can utilize either standard circuit boards [4] or alumina substrates [5].

An alternate circuit form utilizes lumped-element components that are a small fraction of a wavelength in size and behave as capacitors, inductors, or resistors. The values of the components are independent of frequency over the range of interest. This type of circuit was usually avoided at microwave frequencies in the past because conventional fabrication techniques could not provide coils and capacitors that were sufficiently small to behave as true lumped elements. However, it is now possible to fabricate such elements by use of the technology of line definition developed in the semiconductor industry.

The lumped-element approach always results in smaller circuits than the distributed approach. Although the smaller size may be an

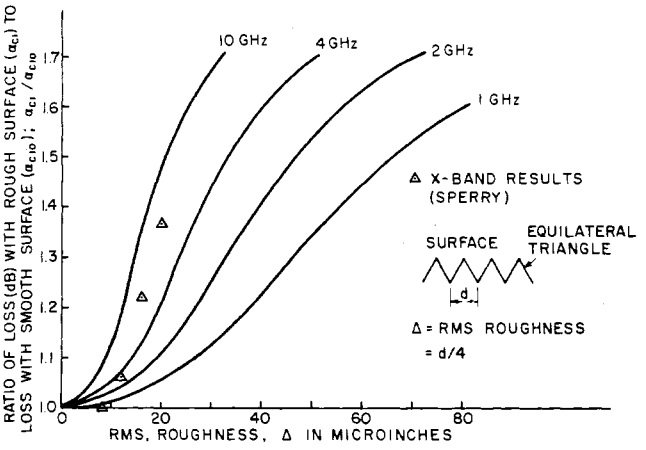

Fig. 4. Ratio of loss of microstrip on rough surface substrate (α_c(dB)) to loss on smooth surface substrate (α_{c10}(dB)) as a function of rms roughness.

advantage in some cases, microstrip circuits are often sufficiently small for most applications. However, there are two key advantages to be gained from the use of lumped-element circuits, both of which are a consequence of small size. These advantages are reduced cost and the adaptability of the lumped-circuit component in a hybrid subsystem.

Because of the small size of lumped-element circuits, many devices can be fabricated simultaneously on a ceramic wafer. As an example, Fig. 3 shows an array of 3-port lumped-element hybrid circuits formed on a 1 by 3/4-in sapphire wafer. The devices are batch-fabricated in the same manner as transistors. Consequently, because optimum use is made of batch-fabrication, the cost of lumped-element circuits tends to be less than that of microstrip lines, which are usually made one at a time.

The passive circuit loss in all forms of MICs will tend to be an order of magnitude higher than the loss in conventional circuits. This increased loss is primarily due to the great reduction in conductor surface area.

Technology of Hybrid MICs

Two types of hybrid technologies have evolved for low-frequency circuits, the thick-film and thin-film approaches. The general names thick and thin films cannot be applied in microwave applications since, regardless of technology used, conductor films must be of the order of three to five skin depths thick. However, the processes used for the two technologies can be considered for microwave circuits. The low-frequency thick-film conductor approach involves the application of a paste containing metal particles to a substrate and the subsequent firing of the film. The conductor pattern may be defined by printing the paste through a screen or by etching after the film is fired. The low-frequency thin-film approach involves the vacuum deposition of a thin film by evaporation or sputtering. The conductor patterns are usually defined by etching. Plating may be used in both techniques to increase the conductor thickness to be required three to five skin depths.

The fired films require a glass phase in the ceramic substrate for adhesion to the substrate. This phase is usually not present in high-quality microwave substrates such as the 99.5-percent body alumina; however, it is present in the lower purity substrates. Therefore, in order to achieve good adherence of fired films to substrates, it may be necessary to use a mechanical bond which can be obtained by using a rough surface on the ceramic substrate.

The vacuum deposited films adhere to substrates by a chemical bond that depends on the formation of an oxide between the con-

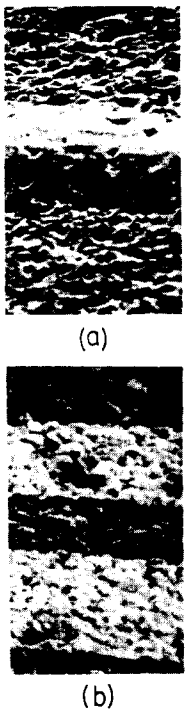

Fig. 5. Scanning electron microscope photographs. (a) Fired Au line on alumina. (b) Deposited Au line on alumina. ×200 magnification.

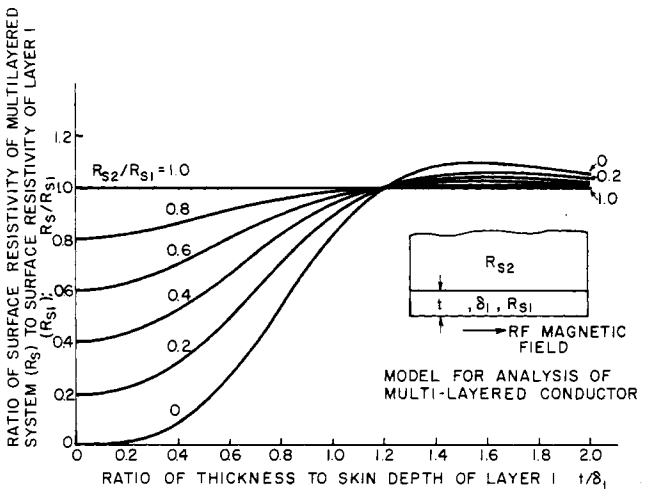

Fig. 6. Ratio of surface resistivity of multilayered system (R_s) to surface resistivity of adhesion layer (R_{s1}) as function thickness of adhesion layer (t/δ_1).

ductor and the substrate. The oxide is usually formed in a thin layer of a relatively high-resistivity metal as chromium, titanium, or tantalum. The chemical bond can be formed on a very smooth substrate surface.

There are several factors that make the deposited metal approach considerably more desirable for microwaves than the fired metal technique. These include substrate surface finish, metal film conductivity, and film porosity. These factors result in higher loss and poorer definition in a fired film than in a deposited film.

The effect of surface roughness on microwave loss was studied twenty years ago by Morgan [6]. Theoretical eddy current losses for equilateral triangular grooves, transverse to current flow, were derived from Morgan's work and are shown in Fig. 4. Also shown in Fig. 4 are the experimental data presented by Sperry Rand, Inc., [7]. The correlation between theory and experiment is good, in spite of the neglect of grooves parallel to current flow. It is apparent from Fig. 4 that rms surface finishes of the order of 5 micro-inches or less are required at X band if the percentage increase in loss (decibels) due to rough surfaces is to be kept below 5 percent. An rms surface finish of 10–20 micro-inches is suitable at L band. Since rougher surfaces are often used in order to achieve a fired-film mechanical bond, the loss of the fired-film line for X-band applications will tend to be considerably higher (40–65 percent) than the deposited film line on a smooth substrate. Fired films have been used on lower purity alumina substrates with 5–10-microinch finish, but these substrates tend to introduce more loss than the 99.5 percent body alumina.

The dc conductivity of the fired film (thick film) lines tends to be significantly less than the bulk metal. As an example, fired gold lines may have conductivities as low as 10 percent of the conductivity of bulk gold. Fig. 5(a) shows a photomicrograph of a fired film gold line. The rough texture and the structure due to suspended metal particles in the glass phase is evident. The relatively smooth texture of the deposited film is illustrated in Fig. 5(b). The conductivity of an evaporated and plated gold film is usually greater than 50 percent of the bulk conductivity of gold. Accordingly, the loss of the fired film may be up to 2.5 times higher than the loss of the deposited film.

The structure of the fired film is relatively "porous" as illustrated in Fig. 5(a). It is difficult to achieve straight edges with this type of film and the ragged edges and hemispherical shape of the conductors contribute to loss. Etching of fired films is rather difficult since the film is a two-phase system and both a glass etch and a metal etch must be used. The fired film system cannot be used for lumped elements or high impedance lines where extremely fine resolution is required.

Experimental results [8], [9] on fired film microstrip lines have tended to confirm the high loss and, in general, the loss measured is two times the loss of a similar deposited film line. For this reason, the bulk of the microstrip work has been done with deposited metal systems on smooth substrates.

The thin film of high resistivity metal used for adhesion is a source of additional loss in the deposited metal system. The loss of the multilayered metal system shown later in Fig. 7 may be calculated by an extension of the analysis presented by Ramo and Whinnery [10]. The real part of the surface impedance R_s of the multilayered metal system is given by

$$R_s = R_{s1}\frac{\left[1+\frac{R_{s2}}{R_{s1}}\right]^2\exp(4t/\delta_1)+2\left[\left(\frac{R_{s2}}{R_{s1}}\right)^2-1\right]\sin\frac{2t}{\delta_1}-\left[\frac{R_{s2}}{R_{s1}}-1\right]^2}{\left[1+\frac{R_{s2}}{R_{s1}}\right]^2\exp(4t/\delta_1)-2\left[\left(\frac{R_{s2}}{R_{s1}}\right)^2-1\right]\cos\frac{2t}{\delta_1}+\left[\frac{R_{s2}}{R_{s1}}-1\right]^2} \tag{1}$$

where

R_{s1} surface resistivity of film 1 (adhesion layer)
R_{s2} surface resistivity of film 2 (conductor)
t thickness of film 1
δ_1 skin depth of film 1.

Equation (1) is plotted in Fig. 6 for a range of resistance ratios. The increased loss in a chromium-gold microstrip system over the pure

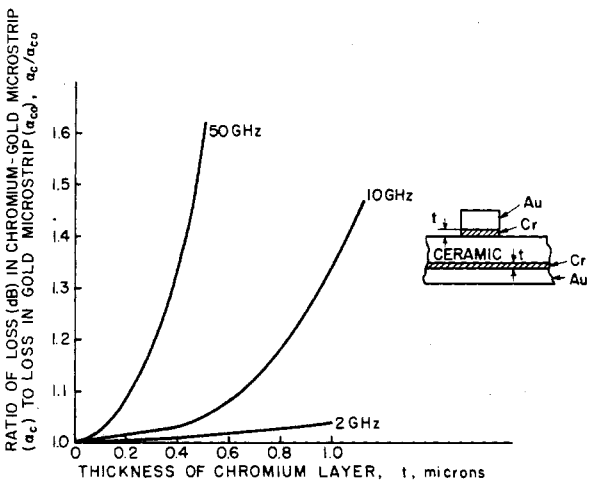

Fig. 7. Ratio of loss (α_c) of Cr–Au microstrip to loss of Au microstrip (α_{co}) as function of Cr thickness.

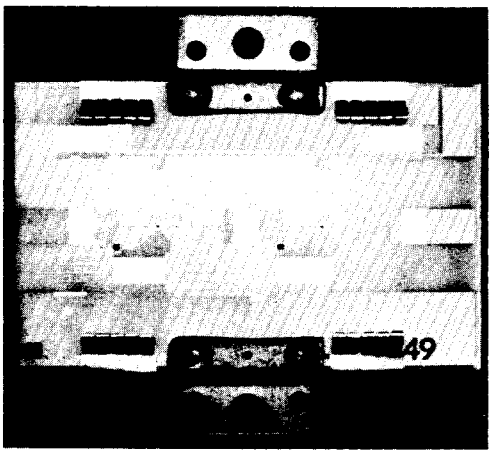

Fig. 8. Two-stage L-band transistor amplifier with tantalum nitride resistors and interdigitated capacitors. (Courtesy of Bell Laboratories, Inc.)

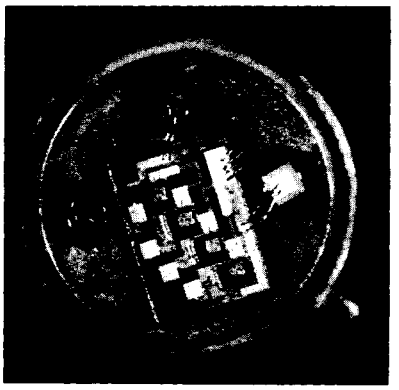

Fig. 9. Four-stage transistor low noise broad-band amplifier (70–700 MHz) with NiCr resistors and SiO_2 capacitors.

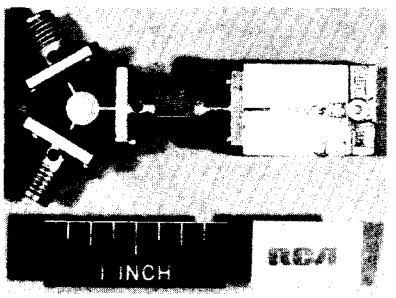

Fig. 10. X-band transferred electron amplifier with GaAs diode and circulator; 2-GHz bandwidth, 12-dB gain.

gold microstrip system [11] is shown in Fig. 7. The calculations account for the change in resistivity of the thin chromium films as a function of thickness of the film [12]. Chemical bonds are achieved with adhesive layers from 100–500 Å thick. Hence the typical adhesion layer will produce only a negligible increase in loss at frequencies well into the millimeter bands.

Deposited Film Systems

There are a variety of metal systems that may be used for deposited film circuits. The choice of a system is determined by the particular passive elements required in a circuit, the temperature range that the circuit will be subjected to during processing and operation, the compatability with the active devices and in some cases the availability of processing equipment. The tantalum system [13] offers the possibility of producing capacitors, resistors, and rudimentary interconnections (subsequently plated up with a high conductivity conductor) with a single material. Other refractory materials, notably hafnium and titanium, may be similarly used; however, none have achieved the success of the tantalum system to date. Tantalum and many of its compounds are very stable and can be anodized to form dielectric films and can be reactively sputtered to form resistive films. The tantalum films are usually sputtered onto a substrate. Tantalum pentoxide (Ta_2O_5) capacitors and tantalum nitride (Ta_2N) resistors have been made with extremely fine accuracies. The L-band transistor amplifier fabricated by Bell Laboratories, shown in Fig. 8, is an example of a tantalum system MIC. Interdigitated capacitors [14] with a Ta_2O_5 flash are utilized. The conductors are gold plated over a layer of tantalum.

Alternative metal systems based on evaporated chromium or titanium as the adhesion layer are very common. The following systems are metal layer combinations that have been successfully used.

Cr–Au

Cr–Cu–Au

Cr–Cu

Cr–Cu–Ni–Au

Ti–Pd–Au

Ti–Pt–Au.

The gold top surface is excellent for ultrasonic bonding, while the copper top surface usually requires soldering for bonding. The Ti–Pd–Au system is metallurgically stable under high temperature conditions while the Cr–Au system will result in a high resistivity conductor if exposed to elevated temperatures for long periods.

Evaporated nichrome resistors are usually utilized with this metal system. Chromium and titanium resistors do not have the long-term stability of the nichrome resistors. Deposited SiO_2 [15] produced by the pyrolitic decomposition of silane (SiH_4) is a popular dielectric material for MICs based on the above metal systems.

Fig. 9 is a broad-band (50–700 MHz) amplifier fabricated with SiO_2 capacitors, NiCr resistors, and Cr–Au interconnections. The four transistors are mounted on gold pads with an Si–Sb–Au eutectic and ultrasonically wire bonded with Al wires. Fig. 10 is an X-band transferred electron amplifier utilizing Cr–Cu–Au microstrip lines. A circulator is utilized to separate input and output signals.

TABLE I

CONDUCTOR CHARACTERISTICS

Material	Dc Relative to Cu	Skin Depth δ at 2 GHz (μ)	Surface Resistivity (ohms/square $\times 10^{-7}\sqrt{f}$)	Coefficient of Thermal Expansion (α_T/°C $\times 10^{-6}$)	Adherence to Dielectric Film or Substrate	Method of Deposition[a]
Ag	0.95	1.4	2.5	21	poor	E, Sc
Cu	1.0	1.5	2.6	18	very poor	E, P
Au	1.36	1.7	3.0	15	very poor	E, P
Al	1.60	1.9	3.3	26	very poor	E
W	3.2	2.6	4.7	4.6	good	Sp, EB, V
Mo	3.3	2.7	4.7	6.0	good	EB, Sp
Cr	7.6	2.7	4.7	9.0	good	E
Ta	9.1	4.0	7.2	6.6	very good	EB, Sp
Mo–Mn	5 × Mo				very good	Sc

[a] E = evaporation; EB = electron-beam evaporation; Sc = screening; P = plating ; V = vapor-phase; Sp = sputtering.

TABLE II

PROPERTIES OF DIELECTRIC FILMS

Material	ε_r	Dielectric Strength (V/cm)	Microwave Q
SiO (evaporated)	6–8	4×10^5	30
SiO_2 (deposited)	4	10^7	1000
AL_2O_3 (anodized or evaporated)	7–10	4×10^6	
Ta_2O_5 (anodized or sputtered)	22–25	6×10^6	100
Si_3N_4 (vapor-phase; sputtered)	7.6	10^7	
	6.5	10^7	

TABLE III

PROPERTIES OF RESISTIVE FILMS

Material	Resistivity (ohms/square)	T.C.R. (%/°C)	Stability
Cr (evaporated)	10–1000	−0.1 to +0.1	poor
NiCr (evaporated)	40–400	+0.002 to +0.1	good
Ta (sputtered in A–N)	4–100 +	−0.01 to +0.01	excellent
Cr–SiO (evaporated or cermet)	up to 600	−0.005 to −0.02	fair
Ti (evaporated)	5 to 2000	−0.1 to +0.1	fair

Tables I, II and III summarize the properties of typical metal, dielectric, and resistor materials used for MICs.

SUBSTRATES

Substrates used for MICs must have the following general properties:

1) low loss at microwave frequencies;
2) good adherence for conductors;
3) polished surfaces (2–5-microinch finish) and relative freedom from voids;
4) no deformation during processing of circuit.

The selection of a substrate material also depends on the expected circuits dissipation, the circuit function, and the type of circuit to be used.

Substrates for microstrip circuits should have relatively high dielectric constants (9 or higher) for size reduction. The dielectric constant must be uniform from batch to batch of substrate material and must not vary significantly with temperature.

Substrates with practically no surface voids are used for thin-film lumped-element circuits. In addition, the substrate should be amenable to sawing or scribing for separation of the individual circuits after batch-fabrication.

Compound substrates are occasionally used in MICs for ferrite components or for high thermal-dissipation circuits. Although it is possible to make entire microstrip systems on ferrite substrates, in some applications a ferrite or garnet disk can be inserted in an aluminum substrate. This technique is employed typically when circulators are used in systems. High-power devices require good heat sinks; when the device cannot be mounted directly on a metal heat sink, it may be mounted on beryllium oxide and then electrically connected to a passive circuit fabricated on a lower thermal-conductivity substrate. Fig. 11 is a photograph of a 16-W CW UHF transistor amplifier with the device mounted on a BeO substrate and the lumped-element circuitry on sapphire substrates.

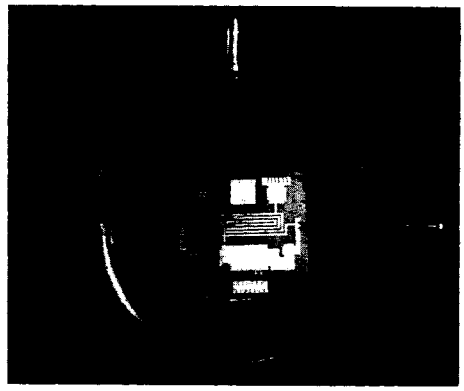

Fig. 11. 16-W 225–400-MHz transistor amplifier. Transistor mounted on BeO substrate. Lumped-element circuits on sapphire substrates.

TABLE IV

PROPERTIES OF SUBSTRATES

Material	Tan at 10 GHz	ε_r	k (W/cm · °C)	Applications
Alumina	2×10^{-4}	9.6–9.9	0.2	microstrip, suspended substrate
Sapphire	10^{-4}	9.3–11.7	0.4	microstrip, lumped element
Glass	4×10^{-4}	5	0.01	lumped element
Beryllium oxide	10^{-4}	6	2.5	compound substrates
Rutile	4×10^{-4}	100	0.02	microstrip
Ferrite/garnet	2×10^{-4}	1316	0.03	microstrip, slot line, coplanar compound substrates

The properties and applications of some popular substrates are given in Table IV.

The use of high dielectric constant substrates seems appealing as a step towards achieving reduced size circuitry. However, the modal problems discussed in the next section places constraints on substrate thickness with the result that extremely narrow conductors are required for reasonable impedance levels. These narrow conductors tend to be lossy and also introduce severe definition problems. In addition, the dielectric constant of materials such as rutile is quite temperature dependent and this can lead to problems in many applications. For these reasons, materials such as rutile have not been used to any great extent in MICs.

Circuit Design

The designer of MICs does not have the luxury or the ease of trimming or tuning of his circuits once they are fabricated. A cavity or conventional lumped-element circuit can be adjusted and peaked to desired performance with adjustable stubs or capacitors. Since these variable elements are not compatible with MIC technology, the circuit design must be carefully carried out in order to eliminate the need for extensive post-fabrication adjustments. It is therefore important that the properties of the passive and active devices used are well understood.

Theoretical data [16]–[23], suitable for accurate design of microstrip circuits, have been presented only recently even though microstrip lines have been used and studied for nearly twenty years [24].

Microstrip Transmission Line

The fundamental propagation mode of a microstrip line such as that shown in Fig. 1 is TEM. At low microwave frequencies, most of the energy propagates in the dielectric below the strip conductor. The remainder of the energy propagates in a fringe field, some of which extends above the dielectric in the air space. The properties of TEM propagation in microstrip can be determined by conformal mapping. The proper mapping to use for microstrip was proposed by Wheeler [1], [17] who derived relationships describing the phase velocity (or effective dielectric constant) and impedance of TEM microstrip propagation. This analysis was carried out for wide strips (width of strip conductor w to thickness of dielectric layer h ratio greater than unity) and for narrow strips (w/h less than unity). The phase velocity V_{ph} in terms of the effective dielectric constant ε_{reff} is given as

$$V_{ph} = \frac{3 \times 10^{10}}{\sqrt{\varepsilon_{reff}}} \quad \text{(cm/s)}. \tag{2}$$

The effective dielectric constant is expressed in terms of a dielectric filling factor q as

$$q = \frac{\varepsilon_{reff} - 1}{\varepsilon_r - 1} \tag{3}$$

where ε_r is the dielectric constant of the insulating layer.

The dielectric filling factor for wide strips is given by

$$qd = d - \ln\frac{d+c}{d-c} + \frac{0.732}{\varepsilon_r}\left[\ln\frac{d+c}{d-c} - \cosh^{-1}(0.358d + 0.595)\right] + \frac{\varepsilon_r - 1}{\varepsilon_r}\left(0.386 - \frac{1}{2(d-1)}\right) \tag{4}$$

where $d = 1 + \sqrt{1+c^2}$ and c is found implicitly from

$$\frac{\pi w}{2h} = c - \sinh^{-1} c$$

where w is the width of the strip conductor and h is the thickness of the dielectric. The impedance of the wide strip line is given as

$$Z_0 = \frac{377\,h}{\sqrt{\varepsilon_r}\,w}\left[1 + \frac{h}{\pi w}\left\{2\ln 4 + (\varepsilon_r + \frac{(\varepsilon_r+1)}{\varepsilon_r}\ln\frac{\pi e}{2}\left(\frac{w}{2h} + 0.94\right) + \frac{\varepsilon_r - 1}{\varepsilon_r^2}\ln\frac{e\pi^2}{16}\right\}\right]^{-1} \tag{5}$$

For the narrow strip case, Wheeler shows that the effective dielectric constant is

$$\varepsilon_{reff} = \frac{\varepsilon_r + 1}{2}\left(1 + \frac{\varepsilon_r - 1}{\varepsilon_r + 1}\,\frac{\ln\frac{\pi}{2} + \frac{1}{\varepsilon_r}\ln\frac{4}{\pi}}{\ln\frac{8h}{w}}\right) \tag{6}$$

and the impedance is

$$Z_0 = \frac{377}{2\pi\sqrt{\frac{\varepsilon_r+1}{2}}}\left[\ln\frac{8h}{w} + \frac{1}{8}\left(\frac{w}{2h}\right)^2 - \frac{1}{2}\,\frac{\varepsilon_r - 1}{\varepsilon_r + 1}\left(\ln\frac{\pi}{2} + \frac{1}{\varepsilon_r}\ln\frac{\pi}{4}\right)\right]. \tag{7}$$

Wheeler also presents implicit equation for deriving the h/w values in terms of the desired impedances. This type of data can be very useful for computer aided design. For the wide line,

$$\frac{w}{h}\,\frac{\pi}{2} = \frac{377\pi}{2\sqrt{\varepsilon_r}\,Z_0} - 1 - \ln\left(\frac{377\pi}{\sqrt{\varepsilon_r}\,Z_0} - 1\right) + \frac{\varepsilon_r - 1}{2\varepsilon_r}\left[\ln\left(\frac{377\pi}{2\sqrt{\varepsilon_r}\,Z_0} - 1\right) + 0.293 - \frac{0.517}{\varepsilon_r}\right] \tag{8}$$

and for the narrow line,

$$2\frac{h}{w} = \frac{1}{4}e^{h'} - \frac{1}{2}e^{-h'}$$

where

$$h' = \sqrt{\frac{\varepsilon_r+1}{2}}\,\frac{Z_0}{60} + \frac{\varepsilon_r - 1}{\varepsilon_r + 1}\left(0.226 + \frac{0.120}{\varepsilon_r}\right). \tag{9}$$

Curves [18] of impedance and wavelength are shown in Figs. 12 and 13.

Some recent work has been presented on a wave analysis [21], [22] of microstrip propagation. A microstrip line was enclosed in a metal container and a mixed TE and TM solution was used. The use of the metal walls permits a straightforward specification of boundaries, certainly simpler to handle than the open boundaries of a microstrip in free space. The enclosed line is practical since most circuits will be used in a package. Microstrip propagation is analyzed by moving the metal walls far from the line. This analysis has shown that the wavelength based on a dispersion-free TEM solution may be as much as 5 percent too high at 10 GHz, but will be correct in the 2-to-3-GHz range and below.

The loss per unit length of a microstrip line [18] can be shown to be inversely proportional to the substrate thickness h; consequently, the Q_0 (unloaded Q) of a microstrip resonator is directly proportional to h. Furthermore, a TEM analysis shows the Q_0 attainable for microstrip resonators to be proportional to the square root of

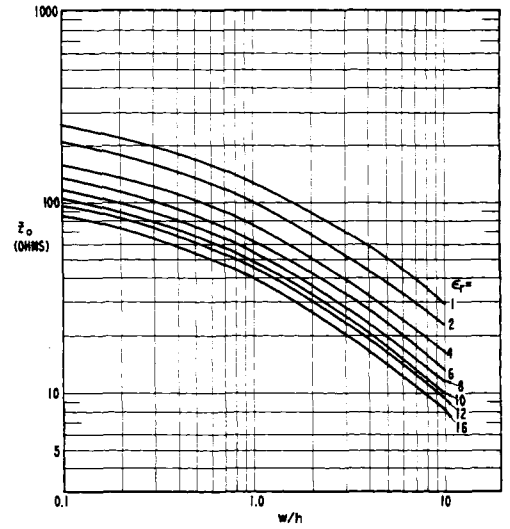

Fig. 12. Impedance of microstrip as function of width of conductor to thickness of substrate.

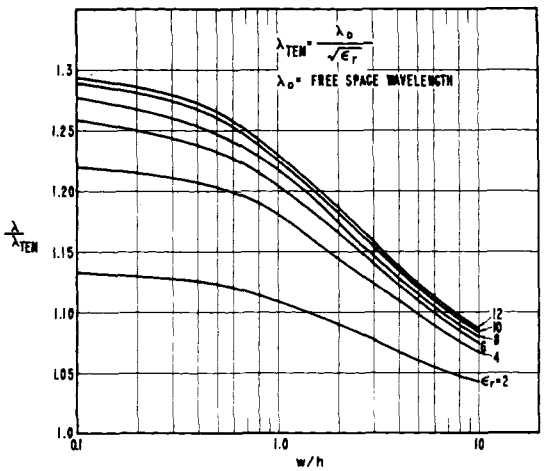

Fig. 13. Normalized guide wavelength of microstrip as function of width of conductor to thickness of substrate.

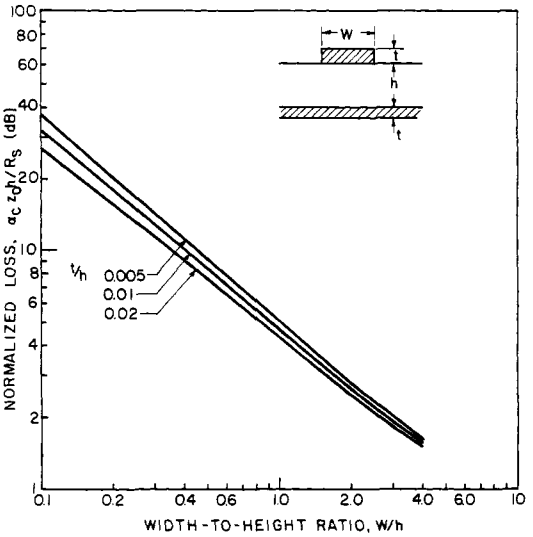

Fig. 14. Normalized loss of microstrip as function of width of conductor to thickness of substrate (after Pucel, Massé, and Hartwig [23]).

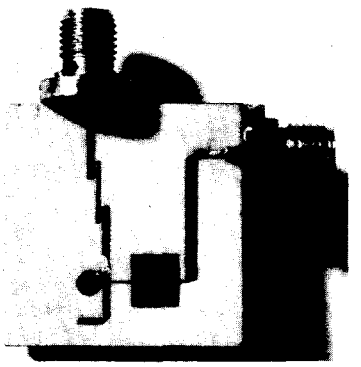

Fig. 15. Times 4 multiplier (2.125 GHz to 8.5 GHz) with low-pass filter, coupled line bandpass filter and open circuit idler stub.

frequency. Quarter-wave resonators on 25-mil-thick alumina substrates have Q_0 values of about 200 at 2 GHz, while Q_0 of about 400 is achievable at 10 GHz using 50-Ω resonators. Lower impedance lines will yield higher Q_0 values.

Theoretical curves of loss of microstrip line have been presented and verified by Pucel *et al.* [23], and are reproduced in Fig. 14. The loss per wavelength of the TEM line has been shown by Caulton *et al.* [18], to be independent of dielectric constant to a first approximation.

There are a number of higher order modes that can exist in microstrip. The presence of the metal enclosure used in practice and in the analysis will alter many of these modes. A particular family, surface modes can be easily excited when using high dielectric constant substrates unless precautions are taken. The cutoff frequency of the lowest order TE_1 surface mode is [25]

$$f_{TE_1} = \frac{3 \times 10^{10}}{4h\sqrt{\varepsilon_r - 1}}, \qquad h \text{ in cm} \tag{10}$$

which occurs when the substrate thickness is approximately $\lambda_0/(4\sqrt{\varepsilon_r})$.

In order to avoid working near this cutoff, relatively thin substrates must be used with high dielectric constant substrates. Consequently, in order to achieve reasonable high impedance levels, extremely narrow lines will be required and this, in turn, leads to definition problems.

Open-circuit microstrip stubs are frequently used in filters and matching networks as shown in the idler circuit of the times four multiplier illustrated in Fig. 15. An ideal lossless stub with a true open-circuit loading presents a pure susceptance at the junction of the stub and the main line.[1] However, the actual boundary condition at the open end of the line is not an open circuit but instead is a complex load that can be represented by a conductance G due to radiation of the principal mode and a susceptance B due to energy stored in the higher order modes. Because of the complex load and distributed losses in the stub, the actual stub admittance presented at the junction of the stub and the main line, is complex.

The susceptance at the open end B can usually be represented by a hypothetical extension Δl of the stub, where Δl is approximately 0.3 to 0.5 substrate thickness [26]. The simple theory for infinitely wide plates results in an extension of 0.44 h.

The radiation conductance can be calculated by treating the problem as radiation from an aperture [27]–[30]. Sobol [27] has shown that the conductance G can be approximated as

$$G \approx \frac{\sqrt{\varepsilon_{reff}}}{180}\left(\frac{w}{\lambda}\right)^2 = \frac{(\varepsilon_{reff})^{3/2}}{180}\left(\frac{w}{\lambda_0}\right)^2. \tag{11}$$

[1] The exact location of the junction will not coincide with the geometric junction but may be displaced by a distance of the order of the substrate thickness.

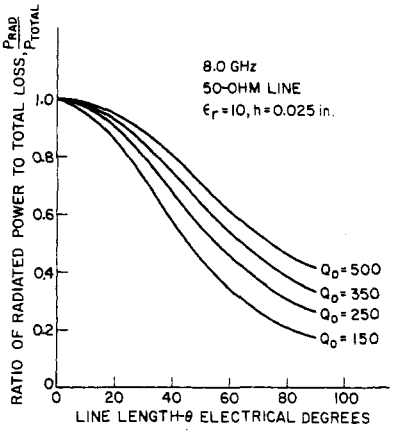

Fig. 16. Ratio of radiated power to total loss of open microstrip stub as function of stub length.

The ratio of the losses due to radiation to the total stub losses at 8 GHz is plotted in Fig. 16 for a 50-Ω line on a 0.025-in thick alumina substrate as a function of stub length. This plot illustrates the importance of considering radiation losses. For a line with $Q_0=250$, 60 percent of the total losses of a 45° line are due to radiation while 30 percent of the total losses of a 90° line are due to radiation. The value of B used is taken from the results of Napoli and Hughes [26], where $\Delta l \approx 0.4\,h$.

The ratio of the radiation losses to the distributed losses of a quarter-wave resonator is

$$\frac{P_{rad}}{P_{dist}} = \frac{Q_0 Z_0 (\epsilon_{reff})^{3/2} \left(\frac{w}{\lambda_0}\right)^2}{45\pi \left(1 + 4\frac{\Delta l}{h}\frac{h}{\lambda_0}\sqrt{\epsilon_{reff}}\right)}. \tag{12}$$

Fig. 17 shows P_{rad}/P_{dist} for a quarter-wave resonator as a function of the substrate dielectric constant ϵ_r and frequency. The results shown are for a 50-Ω line and are in agreement with the data presented by Denlinger [31].

Lewin [29] considers further cases of radiation from microstrip bends and short circuited stubs.

Microwave circuit elements such as filters, couplers, and hybrids can be made by using coupled microstrip lines. Fig. 15 is an example of an X-band filter fabricated with coupled lines. Several papers [32]–[34] have been published on the coupled microstrip lines. In dealing with these structures, it is necessary to consider the even and odd mode velocities and impedances. It is difficult to achieve high directivity in coupled microstrip lines because of differences between even and odd mode velocities.

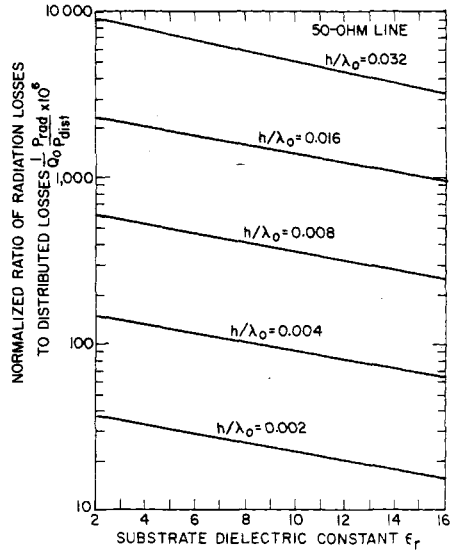

Fig. 17. Ratio of radiated power to distributed loss of open 90° microstrip stub as function of dielectric constant.

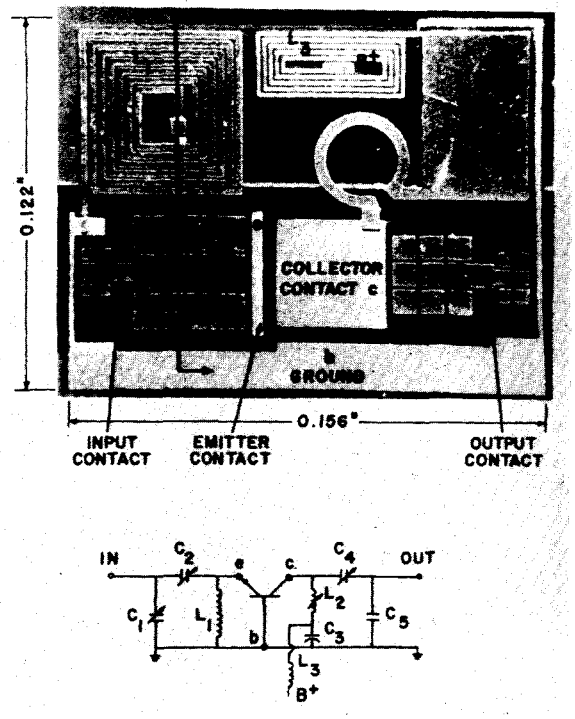

Fig. 18. 1-W S-band lumped-element transistor amplifier.

Lumped-Element Microwave Components

Lumped-element microwave networks are used where small size is desired and in particular for those devices that are to be batch-fabricated. The lumped-element networks can be made in single layer circuits by using interdigitated capacitors and meander line inductors or in three-layer circuits using sandwich capacitors and spiral conductors. The single layer circuits are larger than the three-layer and tend to introduce distributed effects at lower frequencies than the three-layer circuits. Lumped-elements can be combined with microstrip circuits.

In order to exhibit true lumped behavior, a circuit element must be small enough that there is no appreciable phase shift across its entire length. If this requirement is satisfied the low-frequency design equations can be utilized with good success [11], [35]. Fig. 19 is an S-band 1-W transistor amplifier that utilizes rectangular spiral coils as RF chokes, a single turn inductor for tuning and sandwich capacitors. The capacitors are made variable by segmenting the upper plates. In this way the circuit can be tuned over wide frequency ranges by bonding the appropriate capacitors into the circuit at the same time that the transistor is bonded. The amplifier of Fig. 18 is made entirely on a sapphire substrate. A higher power amplifier shown earlier in Fig. 11 is made by using separate input and output circuits on individual sapphire substrates and mounting these substrates and the transistor on a BeO substrate.

When designing a lumped-element network, it is vitally important to account for all parasitic reactance encountered in the circuit. The simplest inductor is a straight strip. The inductance L per unit length of such a structure (in nanohenries per centimeter) is given by [35]

$$L\left(\frac{\text{nH}}{\text{cm}}\right) = 2\left[\ln\frac{l}{w} + 1.193 + 0.224\frac{w}{l}\right] \tag{13}$$

where l is the length and w is the width of the strip in centimeters.

The resistance r per unit length of the strip inductor (in ohms per centimeter can be determined by assuming that the RF current flow is contained within a skin depth at the upper and lower surfaces of the strip, as follows:

$$r = \frac{\pi K}{w}\sqrt{f \cdot \rho} \tag{14}$$

where f is the frequency in gigahertz, ρ is the resistivity in ohm-centimeters, and w is the width of the strip in centimeters. K is a factor between 1 and 2 which accounts for current crowding at the corners of the strip [35]. The ratio of the Q of the inductor to the total inductance in nanohenries is given by:

$$\frac{Q}{L \cdot l} = 2\frac{w}{l}\frac{1}{K}\sqrt{\frac{f}{\rho}}. \tag{15}$$

A strip inductor is typically used in applications requiring inductances of 0.5 to 4 nH. The strip-conductor equation can be used for a single-turn coil if the width of the strip is much less than the diameter of the turn.

Larger inductance values may be achieved by use of flat spiral inductors. The total inductance L_t of the flat spiral (in nanohenries) is given by:

$$L_t(\text{nH}) = 393\frac{a^2n^2}{8a + 11c} \tag{16}$$

where a is the average radius of the coil in cm.

$$a = \frac{d_0 + d_i}{4}$$

d_0 is the outer diameter in centimeters, d_i is the inner diameter in centimeters, $c=(d_0-d_i)/2$ in centimeters, and n is the number of turns.

It can be shown [35] that the maximum Q of a circular spiral is obtained when the ratio of inner diameter to outer diameter d_i/d_0 is 0.2. For this ratio, Q_{max} of a spiral is expressed as follows:

$$\frac{Q_{max}}{\sqrt{L_t}} = \frac{2.4w}{K}\sqrt{\frac{f}{\rho d_0}} \tag{17}$$

where d_0 and w are in cm, L_t is in nanohenries, f is in GHz, and ρ in ohm-centimeters.

Circular spiral inductors with Q's of 100 at 2 GHz have been fabricated. Square spirals have lower Q values than round spirals, and can be used to obtain the largest inductance in a given area. These inductors are useful for RF chokes. Square spirals 0.080 in on a side have been made with inductances up to 100 nH.

Connection to the center of a spiral coil is usually made by running a section of conductor under the coil. A dielectric film is used to insulate the feedthrough from the main coil winding. The self-resonance of a coil can be estimated as the frequency at which the total unwound electrical length of the spiral (modified by dielectric loading) is one-quarter wavelength.

The inductance equations presented thus far apply to an unshielded inductor. The inductance per unit length is reduced as a ground plane is brought in the vicinity of inductor. The reduction in inductance can be estimated by considering the inductor and the ground as a transmission line. When the characteristic impedance Z_0 of this line is less than $300/\sqrt{\varepsilon_{reff}}$, the effective inductance L_{eff} (in nanohenries) is given by:

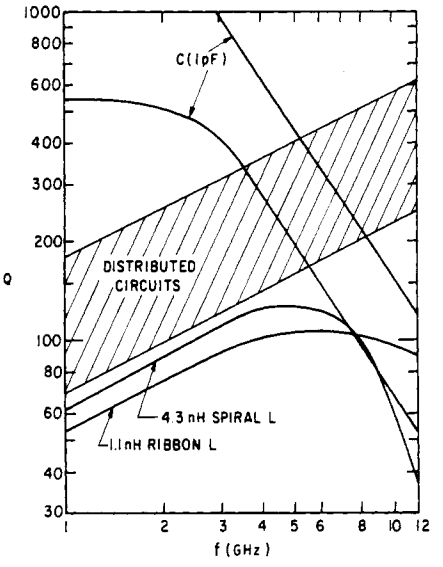

Fig. 19. Q_0 of microstrip resonators and lumped elements as function of frequency.

$$L_{eff} \approx \frac{Z_0\sqrt{\varepsilon_{reff}} \cdot l}{30} \tag{18}$$

where l is in centimeters.

To obtain the unshielded inductance value, it is necessary that the distance to a ground plane beneath an inductor on alumina or sapphire be greater than 20 times the width of the inductor conductor. Similarly, a ground in the same plane as the inductor should be five widths away.

A capacitor may be considered as a short length of the transmission line with an open-circuit load. The driving point impedance of this structure is given by:

$$Z_m = \frac{2R_0}{3} + \frac{1}{Q_d\omega C_0} - j\frac{1}{\omega C_0} \tag{19}$$

where

R_0 = RF resistance of the capacitor plates,
C_0 = parallel plate capacitance,
Q_d = dielectric Q.

Thus the equivalent circuit for a capacitor is two resistors (one representing dielectric loss and the other conductor loss) in series with a capacitor. The total Q of the capacitor is given by:

$$Q_{total} = \frac{Q_dQ_s}{Q_d + Q_s} \tag{20}$$

where

$$Q_s = \frac{3}{2\omega C_0R_0}.$$

Generally the dielectric Q or Q_d of most materials varies little with frequency in the microwave range, while Q_s varies inversely as the product of frequency to the three halves and capacitance. Typical Q_0 values for microstrip [36] and lumped-element components are shown in Fig. 19.

Active Devices

Active devices can be mounted in MICs in a variety of ways. The most common method is to mount the semiconductor chip directly in the circuit, using the same technique as in mounting a device in a package. Examples of this mounting are shown in Figs. 8, 9, 11, and 18. The transistors are eutectic mounted on gold pads and wire bonds are used to connect the circuit to the device contacts. Usually several bond wires are used in parallel to reduce the parasitic inductance. For devices with large contact area, it is possible to use thermo-compression bonding and foil in place of the wire bonds. Shunt-mounted devices can be mounted directly on ground (thermal and electrical) or on posts to achieve good thermal mounts. Beam leads provide an excellent mounting scheme for low dissipation microwave devices and both diodes and transistors have been mounted using this technique. However, this technique has inherent thermal limitations and cannot be used for power devices.

An alternate for incorporating devices into circuits is to use a chip carrier [37] as illustrated in Fig. 20. The transistor carrier of Fig. 20 is used for *L*-band applications and has excellent thermal properties. The carrier has specific lengths of transmission line on the emitter and collector leads to provide impedance transformation to a specific level. The carrier is mounted in a microstrip circuit and foils are used to connect the carrier to the circuit.

In many cases the entire circuit will be enclosed in a hermetic package so that it may not be necessary to use hermetic chip packages for the devices. In other applications, hermetic chip packages are required. A hermetic package suitable for microstrip circuits is shown in Fig. 21.

As mentioned previously, tuning of MICs after fabrication is difficult and it is important to obtain accurate characterization of devices. One of the more difficult problems in device characterization is the definition of reference planes. It is important to characterize the device in a fixture that closely approximates the final circuit to avoid shift in reference planes in going from the text fixture to a circuit. The test fixtures must be completely characterized to account for all parasitics.

Scattering parameters are convenient to use for the design of linear circuits. Because these parameters are determined with ports terminated in 50 Ω rather than an open or a short circuit, many of the stability problems encountered in *y* and *z* characterizations are eliminated.

In the design of nonlinear circuits, such as power amplifiers, the linear circuit analysis cannot be used and it is necessary to measure the device parameters under dynamic conditions at the desired frequency and power level. A system such as that shown in Fig. 22 can be used for this measurement. The stubs are used to tune the device to the desired operating points. The device jig is removed, and the impedance presented at the device plane is then determined. A circuit is synthesized to approximate the required impedances over the desired frequency band. The realization of this circuit is then fabricated in either distributed or lumped-element form.

System and Subsystem Applications

The application of MICs for systems and subsystems is illustrated in Figs. 23 and 24. Both figures illustrate modules for phased-array systems. Fig. 23 is the Texas Instruments, Inc., MERA [38] module, which includes a transmitter, receiver, and two phase shifters, including logic. The transmitter input is at *S* band and the output is an 0.7-W pulsed signal at *X* band. Fig. 24 is an RCA *S*-band CW power module [39] that has a 1.5-GHz input and a 12-W 10-percent bandwidth output at 3 GHz.

These are but two subsystem applications of the technology. There are many other modules that have been fabricated incorporat-

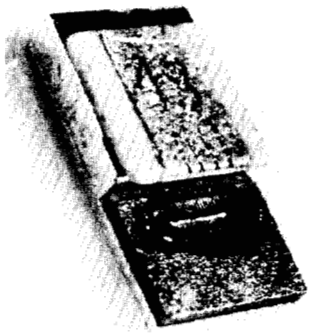

Fig. 20. *L*-band transistor carrier for microstrip applications.

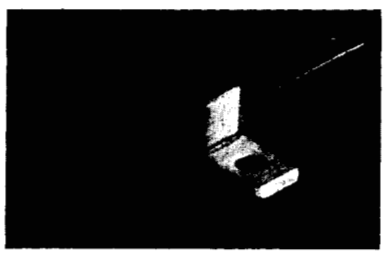

Fig. 21. Hermetic transistor package for microstrip applications.

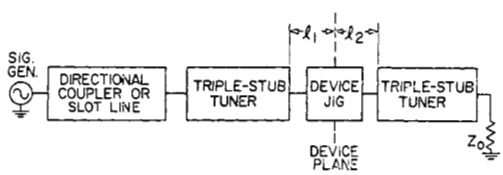

Fig. 22. System for measurement of dynamic characteristics of devices.

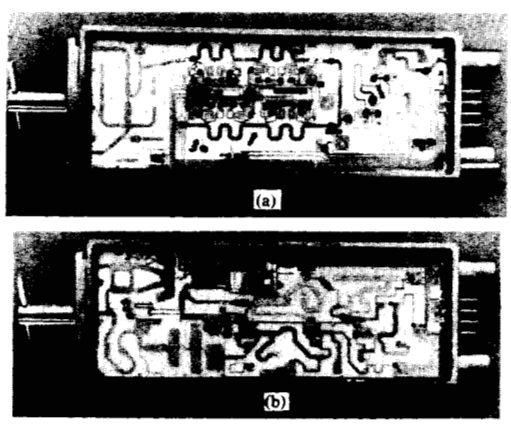

Fig. 23. MERA module. (a) *S*-band preamplifier phase shifters and receiver multiplier. (b) TR switch, mixer, IF amplifier, power amplifier, and multiplier. (Courtesy Texas Instruments, Inc.)

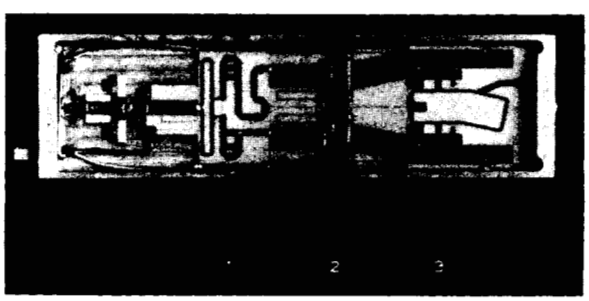

Fig. 24. *S*-band power module including *L*-band preamplifiers, power amplifier, power splitter, multipliers, and combiner.

ing practically every microwave semiconductor device and performing nearly every medium and low-power microwave function.

The designer of modules faces the problem of partitioning the module. He must decide how many functions to include in each block of the module and also what impedance levels are required at the block terminals. There are no general rules at this time for partitioning, each module must be treated individually in terms of economics and performance requirements.

Conclusions

This paper has reviewed various aspects of MICs although there is much that was not covered. The technology has advanced significantly in the past several years and has been met with enthusiasm in the industry. There are problems that remain; however, the prospects are for a bright future. In addition, the technology developed has application in other areas of the microwave industry. As an example, the techniques for depositing microstrip lines on ceramic can be used for planar circuits for vacuum traveling-wave amplifiers. In addition, deposited circuits are currently being used for surface wave acoustic devices.

Acknowledgment

The author would like to express his gratitude to his colleagues at RCA Solid State Division, Somerville, N. J.; RCA Microwave Department, Harrison, N.J.; RCA Laboratories and RCA Electronic Components, Princeton, N. J., for many useful discussions and for permission to use their photographs in this paper. The author wishes to thank Dr. M. Caulton for his suggestions and careful reading of the manuscript. Thanks are also due Bell Telephone Laboratories and Texas Instruments, Inc., for permission to exhibit photographs of their microwave integrated circuits.

References

[1] S. B. Cohn, "Slot-line on alternative transmission medium for integrated circuits," *IEEE G-MTT Int. Microwave Symp. Dig.*, May 1968, pp. 104–109.
[2] C. P. Wen, "Coplanar waveguide, a surface strip transmission line suitable for nonreciprocal gyromagnetic device applications," *IEEE G-MTT Int. Microwave Symp. Dig.*, May 1969, pp. 110–114.
[3] F. C. deRonde, "A new class of microstrip directional couplers," *IEEE G-MTT Int. Microwave Symp. Dig.*, May 1970, pp. 184–189.
[4] B. R. Halford, "Low noise microstrip mixer on a plastic substrate," *IEEE G-MTT Int. Microwave Symp. Dig.*, May 1970, pp. 206–211.
[5] R. S. Englebrecht and K. Kurokawa, "A wide-band low noise *L*-band balanced transistor amplifier," *Proc. IEEE*, vol. 53, Mar. 1965, pp. 237–247.
[6] S. P. Morgan, "Effect of surface roughness on eddy current losses at microwave frequencies," *J. Appl. Phys.*, vol. 20, Apr. 1949, pp. 352–362.
[7] Nonpublished results obtained by Sperry Rand, Inc.
[8] R. N. Patel, "Microwave conductivity of thick-film conductors," *Electron. Lett.*, vol. 6, July 1970, pp. 455–456.
[9] F. Z. Keister, "An evaluation of materials and processes for integrated microwave circuits," *IEEE Trans. Microwave Theory Tech.*, vol. MTT-16, July 1968, pp. 469–475.
[10] S. Ramo and J. R. Whinnery, *Fields and Waves in Modern Radio*. New York: Wiley, 1953, pp. 249–250.
[11] H. Sobol, "Technology and design of hybrid microwave integrated circuits," *Solid-State Technol.*, Feb. 1970.
[12] A. A. Milgram and C. S. Lu, "Preparation and properties of chromium films," *J. Appl. Phys.*, vol. 39, May 1968, pp. 2851–2856.
[13] D. A. McLean, N. Schwartz, and E. D. Tidd, "Tantalum-film technology," *Proc. IEEE*, vol. 52, Dec. 1964, pp. 1450–1462.
[14] G. D. Alley, "Interdigitated capacitors for use in lumped element microwave integrated circuits," *IEEE G-MTT Int. Microwave Symp. Dig.*, May 1970.
[15] N. Goldsmith and W. Kern, "The deposition of vitreous silicon dioxide films from silane," *RCA Rev.*, vol. XXVIII, Mar. 1967, pp. 153–165.
[16] H. A. Wheeler, "Transmission-line properties of parallel wide strips by a conformed-mapping approximation," *IEEE Trans. Microwave Theory Tech.*, vol. MTT-12, May 1964, pp. 280–289.
[17] H. A. Wheeler, "Transmission-line properties of parallel strips separated by a dielectric sheet," *IEEE Trans. Microwave Theory Tech.*, vol. MTT-13, Mar. 1965, pp. 172–185.
[18] M. Caulton, J. J. Hughes, and H. Sobol, "Measurements on the properties of microstrip transmission lines for microwave integrated circuits," *RCA Rev.*, vol. 27, Sept. 1966, pp. 377–391.
[19] C. P. Hartwig, D. Massé, and R. A. Purel, "Frequency dependent behavior of microstrip," *IEEE G-MTT Int. Microwave Symp. Dig.*, May 1968.
[20] H. E. Stinehelfer, "An accurate calculation of uniform microstrip transmission lines," *IEEE J. Solid-State Circuits*, vol. SC-3, June 1968, pp. 101–106.
[21] G. I. Zysman and D. Varon, "Wave propagation in microstrip transmission lines," *IEEE G-MTT Int. Microwave Symp. Dig.*, May 1969, pp. 3–7.
[22] R. Mittra and T. Itoh, "A new technique for the analysis of the dispersion characteristics of microstrip lines," *IEEE Trans. Microwave Theory Tech.*, vol. MTT-19, Jan. 1971, pp. 47–56.
[23] R. A. Pucel, D. J. Massé, and C. P. Hartwig, "Losses in microstrip," *IEEE Trans. Microwave Theory Tech.*, vol. MTT-16, June 1968, pp. 342–350.
[24] F. Assadourian and E. Rimeir, "Simplified theory of microstrip transmission systems," *Proc. IRE*, vol. 40, Dec. 1952, pp. 1651–1657.
[25] R. E. Collins, *Field Theory of Guided Waves*. New York: McGraw-Hill, 1960, pp. 470–474.
[26] L. S. Napoli and J. J. Hughes, "Open-end fringe effect of microstrip lines on alumina," to be published in *RCA Rev.*
[27] H. Sobol, "Radiation conductance of open-circuit microstrip," to be published.
[28] S. Ramo and J. R. Whinnery, *Fields and Waves in Modern Radio*. New York: Wiley, 1953, pp. 526–536.
[29] L. Lèwin, "Radiation from discontinuities in stripline," *Proc. Inst. Elec. Eng.* (London), vol. 107, Feb. 1960, pp. 163–170.
[30] N. Marcuvitz, *Waveguide Handbook*, vol. 10 (Radiation Laboratory Series). New York: McGraw-Hill, 1951, p. 179.
[31] E. J. Denlinger, "Radiation from microstrip resonators," *IEEE Trans. Microwave Theory Tech.* (Corresp.), vol. MTT-17, Apr. 1969, pp. 235–236.
[32] T. G. Bryant and J. A. Weiss, "Parameters of microstrip transmission lines and of coupled pairs of microstrip lines," *IEEE Trans. Microwave Theory Tech.*, vol. MTT-16, Dec. 1968, pp. 1021–1027.
[33] M. K. Krage and G. I. Haddad, "Characteristics of coupled microstrip transmission lines—I: Coupled-mode formulation of inhomogeneous lines," *IEEE Trans. Microwave Theory Tech.*, vol. MTT-18, Apr. 1970, pp. 217–222.
——, "Characteristics of coupled microstrip transmission lines—II: Evaluation of coupled-line parameters," *IEEE Trans. Microwave Theory Tech.*, vol. MTT-18, Apr. 1970, pp. 222–228.
[34] A. Schwarzmann, "Microstrip plus equations adds up to fast design," *Electronics*, vol. 40, Oct. 1967, pp. 109–114.
[35] M. Caulton, S. P. Knight, and D. A. Daly, "Hybrid integrated lumped-element microwave amplifier," *IEEE J. Solid-State Circuits*, vol. SC-3, June 1968, pp. 59–66.
[36] M. Caulton and H. Sobol, "Microwave integrated circuit technology," *IEEE J. Solid-State Circuits*, vol. SC-5, Dec. 1970, pp. 292–303.
[37] E. Belohoubek, D. Stevenson, and A. Rosen, "Hybrid integrated 10-W CW broadband source at *S*-band," *IEEE Int. Solid-State Circuits Conf. Dig. Tech. Papers*, Feb. 1969, pp. 124–125.
[38] T. M. Hyltin, "Microwave integrated electronics for radar and communication systems," *Microwave J.*, vol. 11, Feb. 1968, pp. 51–55.
[39] E. Belohoubek *et al.*, "*S*-band CW power module for phased arrays," *Microwave J.*, vol. 13, July 1970, p. 29.

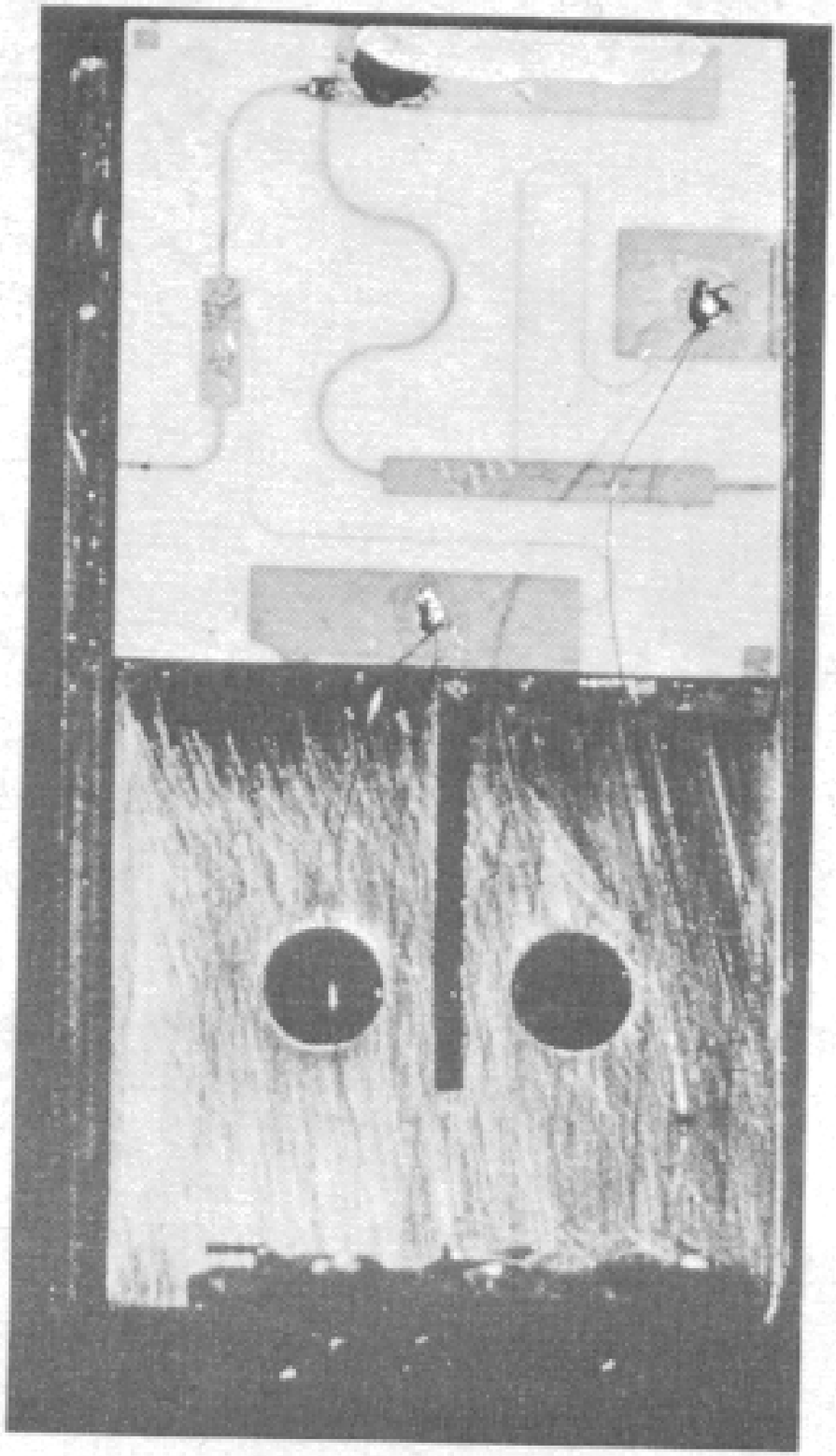

Fig. 1. *L*-band microstrip transistor amplifier, 1 by 1 by 0.010 in alumina substrate, Cr–Au lines and ground plane.

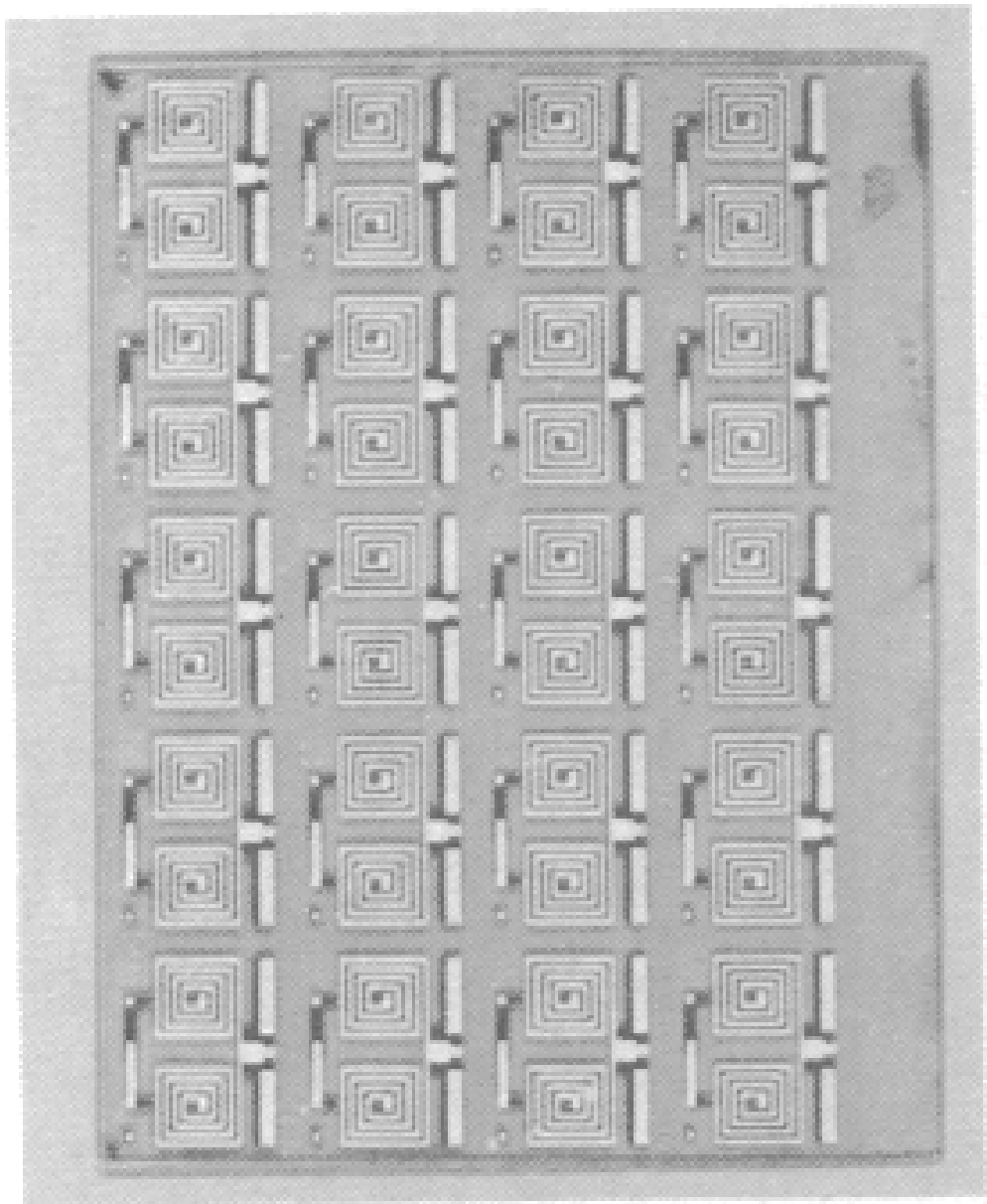

Fig. 3. Array of 3-part UHF lumped element hybrids on 1 by 0.75-in sapphire substrate, Cr–Au lines and inductors and SiO_2 capacitors.

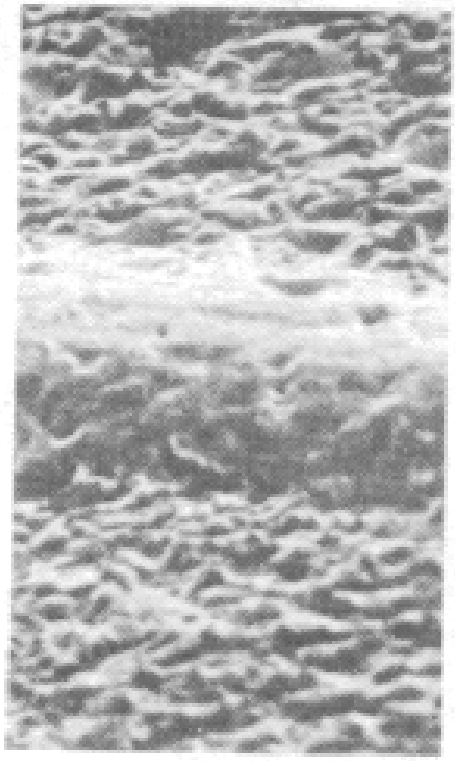

(a)

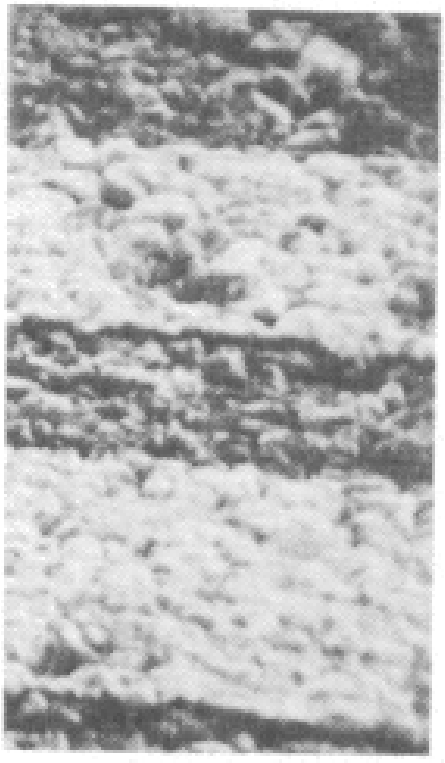

(b)

Fig. 5. Scanning electron microscope photographs. (a) Fired Au line on alumina. (b) Deposited Au line on alumina. ×200 magnification.

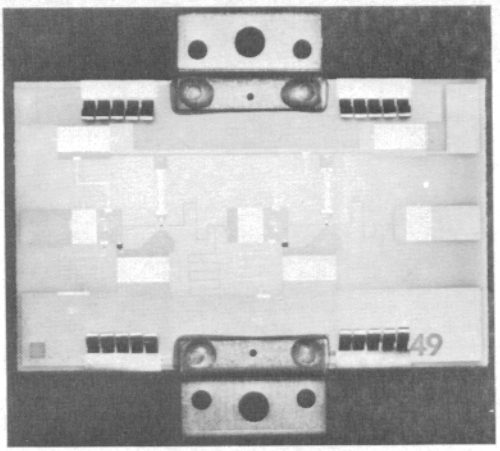

Fig. 8. Two-stage L-band transistor amplifier with tantalum nitride resistors and interdigitated capacitors. (Courtesy of Bell Laboratories, Inc.)

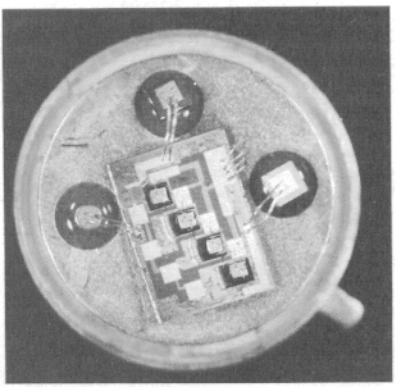

Fig. 9. Four-stage transistor low noise broad-band amplifier (70–700 MHz) with NiCr resistors and SiO_2 capacitors.

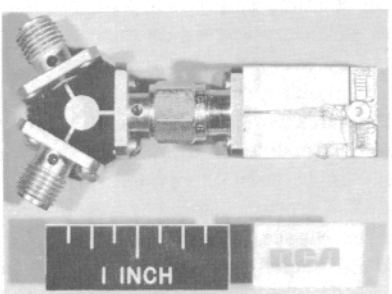

Fig. 10. X-band transferred electron amplifier with GaAs diode and circulator; 2-GHz bandwidth, 12-dB gain.

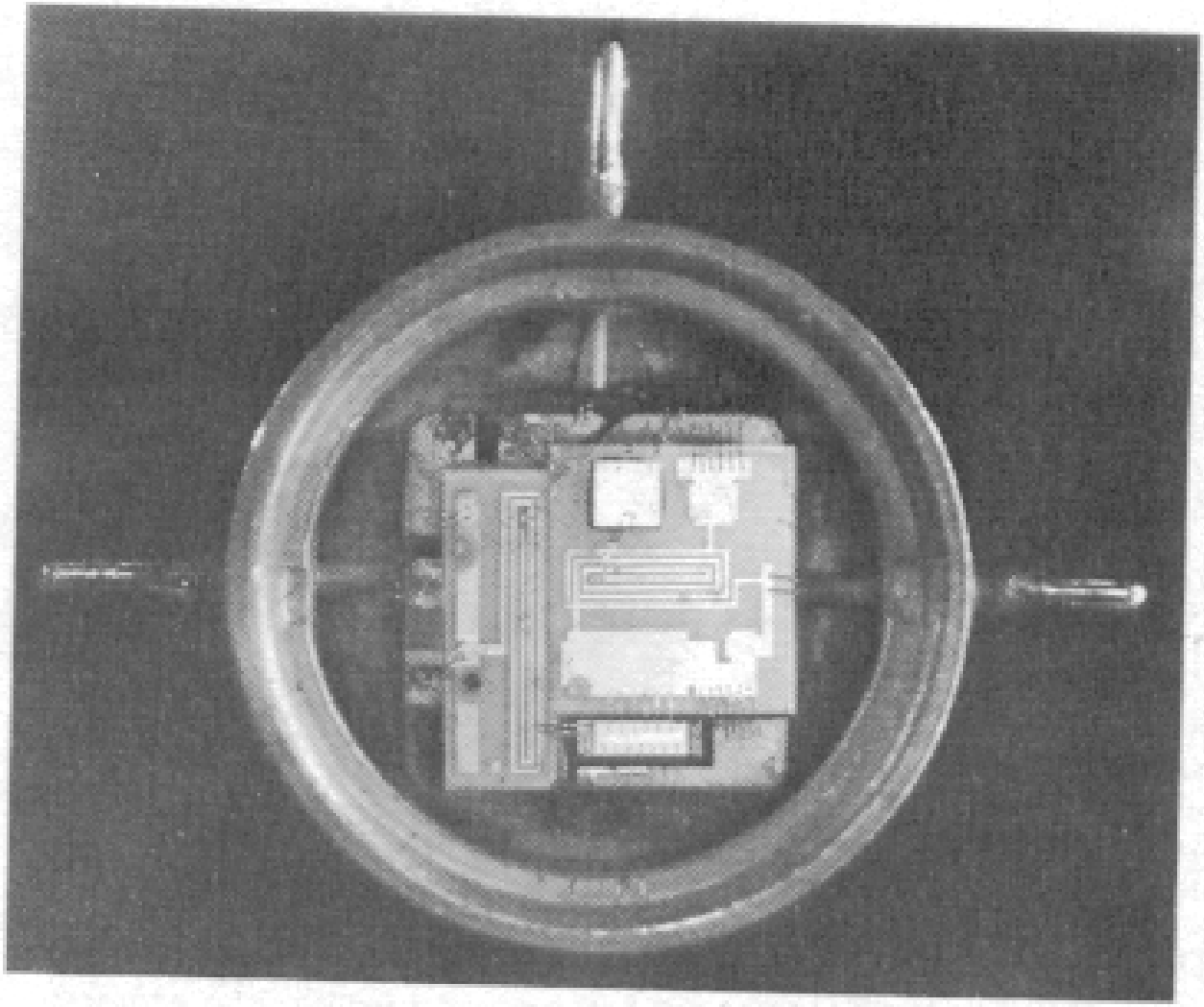

Fig. 11. 16-W 225–400-MHz transistor amplifier. Transistor mounted on BeO substrate. Lumped-element circuits on sapphire substrates.

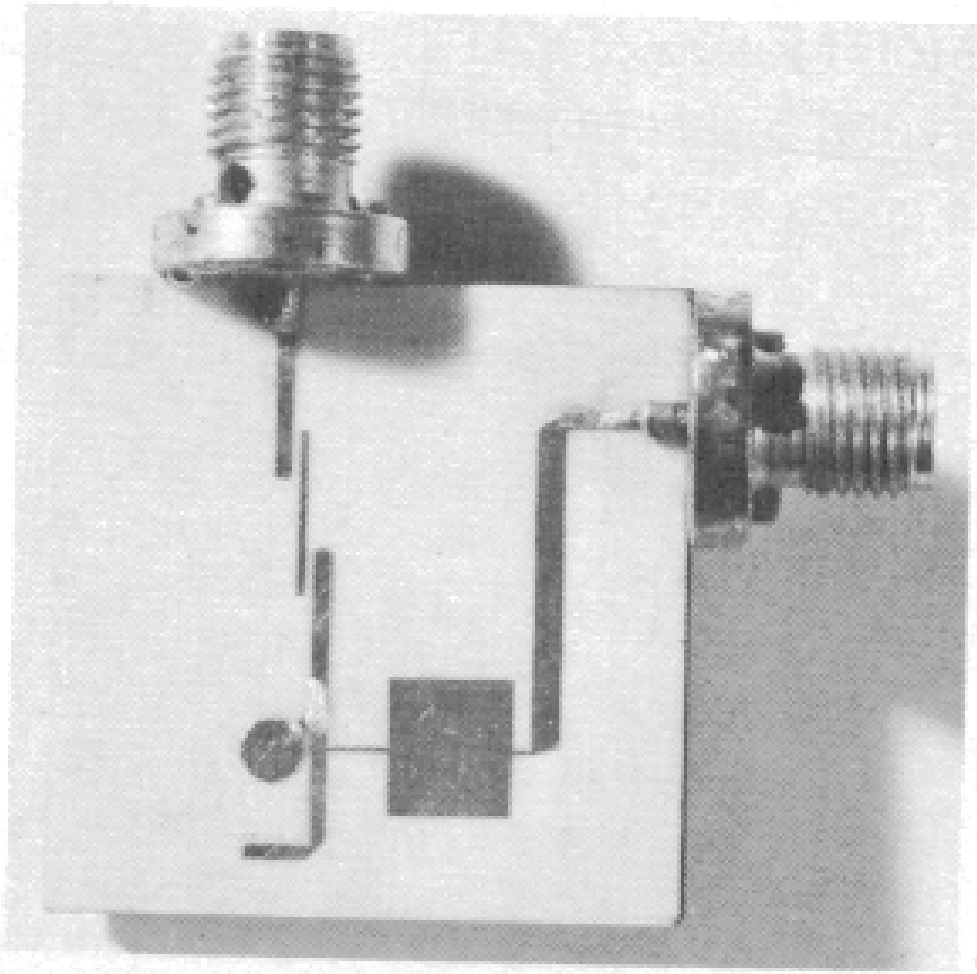

Fig. 15. Times 4 multiplier (2.125 GHz to 8.5 GHz) with low-pass filter, coupled line bandpass filter and open circuit idler stub.

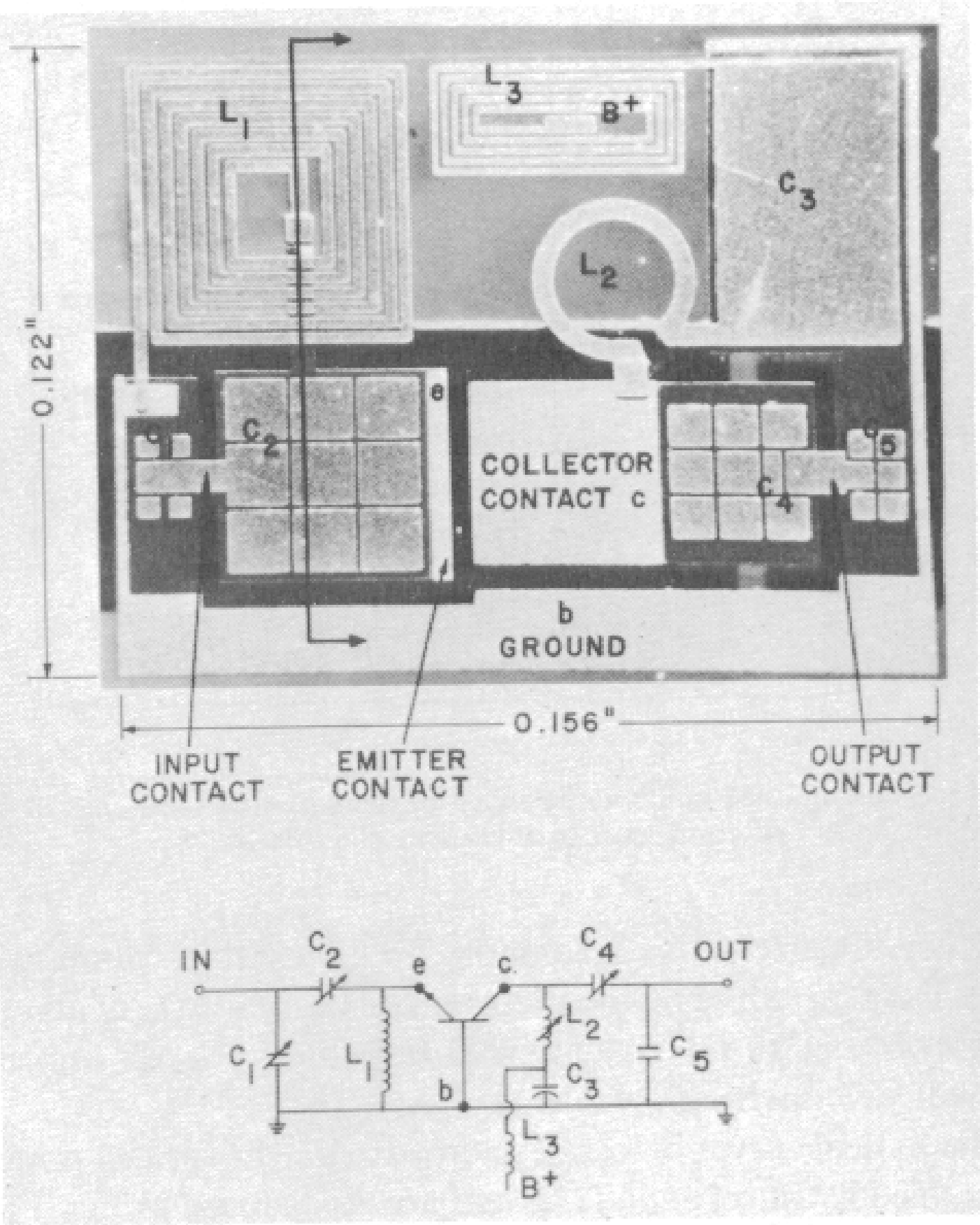

Fig. 18. 1-W *S*-band lumped-element transistor amplifier.

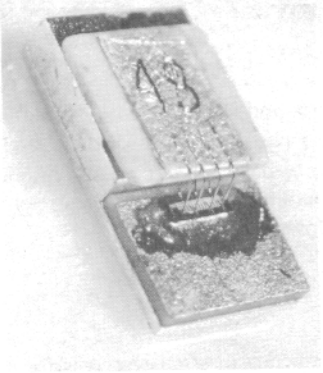

Fig. 20. *L*-band transistor carrier for microstrip applications.

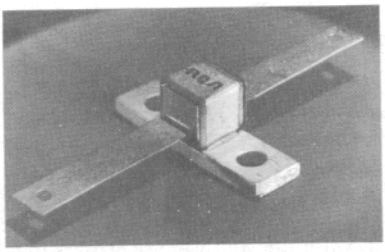

Fig. 21. Hermetic transistor package for microstrip applications.

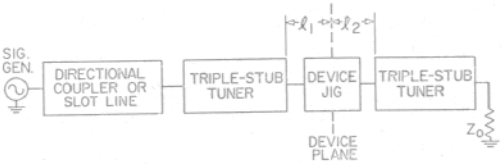

Fig. 22. System for measurement of dynamic characteristics of devices.

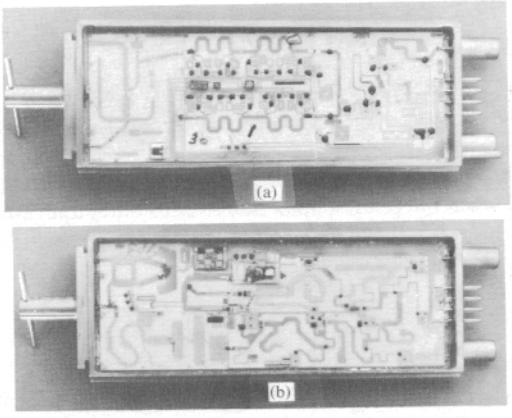

Fig. 23. MERA module. (a) *S*-band preamplifier phase shifters and receiver multiplier. (b) TR switch, mixer, IF amplifier, power amplifier, and multiplier. (Courtesy Texas Instruments, Inc.)

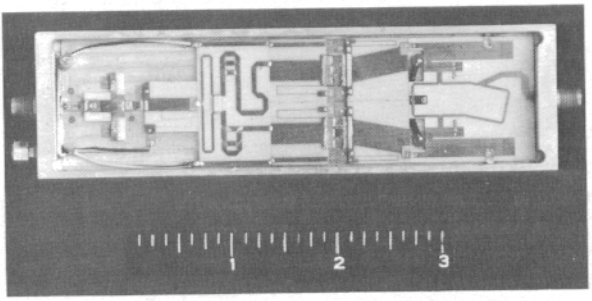

Fig. 24. *S*-band power module including *L*-band preamplifiers, power amplifier, power splitter, multipliers, and combiner.